ISSN 1070-4272, Russian Journal of Applied Chemistry, 2023, Vol. 96, No. 6. pp. 693–701. © Pleiades Publishing, Ltd., 2023.
Russian Text © The Author(s), 2023, published in Zhurnal Prikladnoi Khimii, 2023, Vol. 96, No. 6, pp. 622–631.

Synthesis of Clay-Based Catalysts for the Degradation of Polyolefins by Mechanical Activation

L. V. Furda[a], O. G. Isakulov[a], and O. E. Lebedeva[a],*

[a] *Belgorod State National Research University, Belgorod, 308015 Russia*
**e-mail: olebedeva@bsu.edu.ru*

Received December 4, 2023; revised December 26, 2023; accepted December 29, 2023

Abstract—An assessment was made of the catalytic properties of samples of clay material from the Shebekinskii district of the Belgorod oblast, subjected to mechanical activation during the conversion of a polyolefin–motor oil mixture into liquid hydrocarbons. It was shown that these catalysts under experimental conditions are not capable of converting the polyethylene–motor oil mixture into liquid hydrocarbons, but are very effective in replacing polyethylene with polypropylene. Varying the time of mechanical action on clay materials affects the yield of products of thermocatalytic degradation of polypropylene. The maximum yield of target products (53 wt %) was detected during the thermocatalytic degradation of a polypropylene–motor oil mixture in the presence of a catalyst obtained after grinding the initial clay material for 8 h.

Keywords: degradation of polyolefins, catalysts, mechanical activation, clay material

DOI: 10.1134/S1070427223060095

One of the possible ways to solve the problem of recycling household and industrial plastic waste is converting plastic to hydrocarbons. The use of selective catalysts to produce a mixture of hydrocarbons with a desired range of carbon atom numbers allows the production of liquid products with a composition similar to composition of gasoline or diesel fuel.

Solid acid catalysts are among the most effective in the catalytic conversion of plastics. The process of thermocatalytic transformation using such materials largely depends on the presence of acid sites, the amount and size of catalyst pores [1, 2]. Many works are devoted to the use of synthetic aluminosilicates as catalysts [3, 4]. Microporous zeolite catalysts have active sites with high acidity, inducing skeletal transformations of hydrocarbons [1]. However, the small pore size of zeolites limits the access of large molecules to acid sites located inside the channels. This steric factor brings about a significant yield of gaseous hydrocarbons in the composition of degradation products, since the contact of the polymer chain occurs mainly with the outer surface of the zeolite, where the primary reactions of selective degradation of the polymer, initiated by the surface active sites of the catalyst, proceed.

Inexpensive and available natural aluminosilicates are of great interest as catalysts for the polymer degradation. The high activity and selectivity of clay materials in the degradation of polymers into liquid hydrocarbons compared to microporous zeolites is achieved due to the presence of mesopores in their structure, which increase the availability of acid sites. This mesoporous structure makes it possible to reduce diffusion limitation for the movement of moieties of lower molecular weight macromolecules. Secondary reactions, such as cyclization, aromatization, and disproportionation, induced by medium-strength acid sites, occur inside the pores of the catalyst, which facilitates the selective formation of liquid hydrocarbons [5]. Products fabricated from plastic waste using clay catalysts are often characterized as gasoline and diesel fractions [6–8].

The nature of active sites is almost the same for all types of clays [9]. Original clays in cationic forms usually contain an insufficient number of acid sites. As a rule, to yield catalytically active clays, their chemical activation is used by treating the original clay with acid solutions [10, 11]. Acid treatment removes

Table 1. Chemical composition of clay material

Main components	SiO_2	Al_2O_3	Fe_2O_3	TiO_2	CaO	MgO	Na_2O	K_2O	Total
Content, wt%	54.60	16.08	5.08	0.91	17.80	2.32	0.40	2.81	100.00

mineral impurities, and interlayer cations are replaced by hydrogen ions. Acid activation changes the structure of the clay, resulting in increased specific surface area, greater porosity and increased acidity. This makes it possible to use these materials as effective solid acid catalysts for various transformations.

A fairly large number of works are devoted to the study of the mechanical and mechanochemical activation of clay materials: kaolinite [12], bentonite [13], montmorillonite [14, 15], etc. Mechanochemical activation results in a change in the structure of clay materials, delamination and disorder of layers, and a decrease in crystallite size and changes in the defectiveness of the crystal structure up to complete amorphization of the substance. An increase in the free surface of particles and an enhancing reactivity are also observed. Changes in the crystal structure of surface layers and the appearance of active sites and radicals on the surface determine the specificity of chemical reactions on the activated surface. An increase in the chemical activity of finely ground materials also manifests itself in a rise in catalytic properties, which is explained, on the one hand, by an increase in the specific surface area, and on the other, by an increase in sorption capacity.

There are studies that describe the fabrication of catalysts based on layered clay materials using mechanochemical activation for various chemical processes: the conversion of 1,4-butanediol to 2,3-dihydrofuran [16], the oxidation of α-pinene with *tert*-butyl hydroperoxide [17]. However, in the literature there are no works devoted to the degradation of polymers using mechanically activated clay materials.

This work is aimed at varying the physicochemical properties of clay material by mechanical activation to produce effective catalysts for the degradation of polyolefins into liquid hydrocarbons.

EXPERIMENTAL

Polyethylene film of the Nf(n) grade (JSC BZPI) and disposable polypropylene cups (article no. 170-0022, JSC Standard Plastic Group) were used as samples of polyolefins. Motor oil (density at 15°C 873 kg cm^{-3}, viscosity at 40°C 96.81 $mm^2\ s^{-1}$, viscosity index 160) was used as a solvent for polyolefins.

Catalysts for the degradation of polymers were prepared based on the clay material from the Polyana deposit in the Shebekinskii district of the Belgorod oblast, the chemical composition of which, according to energy-dispersive analysis, is given in Table 1.

According to the results of X-ray diffraction analysis (XRD), this material belongs to polymineral clays. The mineralogical composition is represented by quartz, clinoptilolite, and muscovite (Fig. 1).

Samples of catalysts for the degradation of polyolefins were produced by mechanical activation of clay material. The original clay sample was pre-dried in an oven at 110°C to constant weight. A weighed portion of the dried clay sample was placed in a grinding drum with a 2 L operating volume with corundum cylpebs as grinding bodies of ~15 mm high. Grinding was carried out using a laboratory mill ML-1 equipped with a frequency controller (JSC NPTsK) with a drum rotation speed of 80 rpm. The grinding loading was 35% of the operating volume of the drum. Samples were taken after 1, 2, 4, and 8 h of grinding. The original clay material and the catalysts based thereon resulted from the grinding process are assigned the corresponding indices: G-0, G-1, G-2, G-4, G-8.

The reaction mixture was prepared as follows. A pre-crushed polymer sample and motor oil were placed in a porcelain cup and left for 1 h at room temperature. Next, the mixture was heated to obtain a viscous polymer solution. A sample of catalyst powder was added to the hot solution, mixed, and left at room temperature until solid films were formed. For all samples, the weight ratio of polymer : motor oil : catalyst was 1 : 1 : 1. The resulting solid films were ground to 2–3 mm and loaded into a catalytic reactor.

Experiments on thermocatalytic conversion were conducted in a setup involving a flow-type reactor with a fixed bed of catalyst and reagent. A sample of the

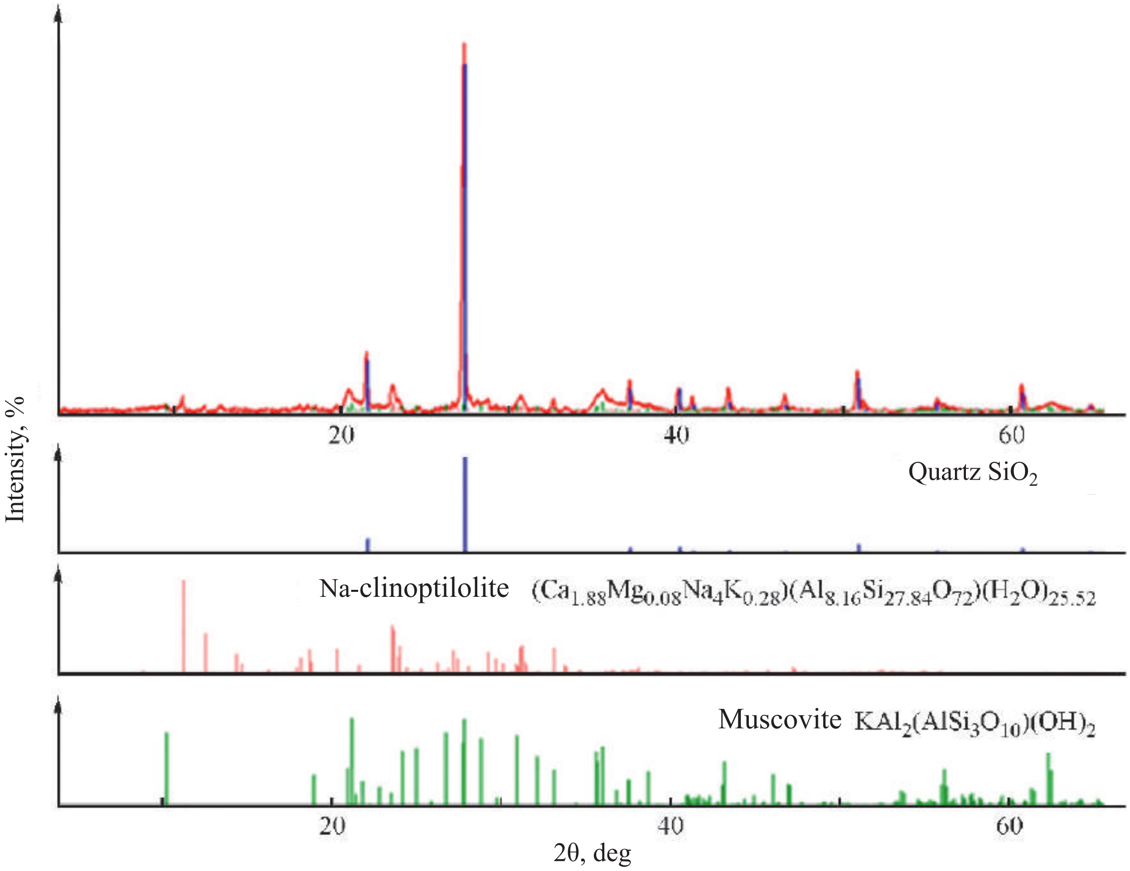

Fig. 1. X-ray powder diffraction pattern of a sample of the original clay material.

reaction mixture in the form of crushed films was placed in the reactor. The temperature was elevated gradually and kept isothermally at 300 or 350°C. Liquid products were collected in a receiver mount at the reactor outlet. The conversion of polymers was carried out in an inert atmosphere of argon. The yield of liquid products (wt %) was calculated taking into account the total weight of the polymer and solvent.

An image of the surface of the original clay material and catalysts based thereon was obtained by scanning electron microscopy (SEM) on a Quanta-200 3D microscope (FEI) at magnifications up to 30 000×. The accelerating voltage at the anode was 20 kV, and the beam current was ~200 mA. The elemental composition of the samples was determined by energy dispersive analysis equipped with an attachment to the specified microscope.

The acid-base properties of the surface of the clay material samples were studied by the Hammett indicator method [18] using the adsorption of monobasic dyes of various types from aqueous solutions with pK_a^x values in the range from +0.80 to +12.80 (Table 2).

Quantitative determination of adsorption sites ($q_pK_a^x$, mmol g^{-1}) of a given acid strength was carried out by the spectrophotometric method on a SPECORD 210 Plus spectrophotometer (Analytik Jena). Solutions were photometered in cuvettes with an absorbing layer thickness of 1 cm relative to the solvent at a wavelength corresponding to the maximum absorption of each indicator (λ_{max}). The content of active sites ($q_pK_a^x$) of a certain acidic strength pK_a^x, was calculated by equation:

$$q_{pK_a^x} = \frac{c_{ind}V_{ind}}{D_0}\left(\left|\frac{|D_0 - D_1|}{m_1} \pm \frac{|D_0 - D_2|}{m_2}\right|\right), \tag{1}$$

where c_{ind} is concentration of the indicator solution (mM); V_{ind} is the volume of the indicator solution taken for analysis (L); D_1 is the optical density of the indicator solution after sorption; D_2 is the optical density of the blank solution; D_0 is the optical density of the indicator

Table 2. Range and some characteristics of acid-base indicators [19]

Indicator name	Acidity index pK_a^x	Wavelength λ_{max}, nm	Concentration of the indicator solution c_{ind}, mM
Crystal violet (analytical grade, Baum-Lux)	+0.80	580	0.599
p-Nitroaniline (analytically pure grade, Interchem Group of Companies)	+1.02	380	0.109
Diamond green (analytically pure grade, Interchem Group of Companies)	+1.30	610	0.320
Fuchsin (base) (part, JSC Reakhim)	+2.10	540	0.299
m-Nitroaniline (analytically pure grade, Vekton JSC)	+2.50	340	0.304
Methyl orange (analytical grade, JSC Reakhim)	+3.46	460	0.281
Bromophenol blue (analytically pure grade, NPP Sintrade Kazan)	+4.10	690	0.045
Methyl red (analytically pure grade, JSC Vekton)	+5.00	430	0.156
Bromocresol purple (analytically pure grade, Interchem Group of Companies)	+6.40	590	0.111
Bromothymol blue (analytically pure grade, Vekton JSC)	+7.30	430	0.195
Phenol red (analytically pure grade, JSC Reakhim)	+8.00	430	0.085
Thymol blue (analytically pure grade, JSC Reakhim)	+8.80	430	0.291
Indigo carmine (analytically pure grade, JSC Reakhim)	+12.80	610	0.077

Table 3. Granulometric composition of the studied catalyst samples

Time of clay material mechanical activation, h	D_{90}[a]	D_{50}[a]	D_{20}[a]	Content of submicrometer fraction <1 μm, %
	μm			
Original sample	42.3	11.3	3.9	0.7
1	36.5	8.6	3.1	0.9
2	35.6	8.0	2.9	0.9
4	31.0	5.9	2.3	1.4
8	28.2	5.3	2.1	1.6

[a] (D_{90}, D_{50}, D_{20}) Particle size below which 90, 50, 20% of the material is contained, respectively.

solution before sorption; m_1, m_2 are the weights of clay sample samples when measuring D_1 and D_2.

The "–" sign corresponds to a unidirectional change in D_1 and D_2 relative to D_0, i.e. D_1 and $D_2 < D_0$ or D_1 and $D_2 > D_0$. The "+" sign corresponds to a multidirectional change in D_1 and D_2 relative to D_0, i.e. $D_1 > D_0$, $D_2 < D_0$ or $D_1 < D_0$, $D_2 > D_0$.

The surface acidity function of the material under study was calculated using the equation

$$H_0 = \Sigma pK_a^x q_{pK_a^x} / \Sigma q_{pK_a^x}. \quad (2)$$

XRD analysis of powders was carried out on a SmartLab X-ray powder diffractometer (Rigaku) with a high-speed D/TEX ULTRA detector using CuK_α radiation. Conditions for recording diffraction patterns: X-ray tube current 250 mA and accelerating voltage 40 kV. Registration was carried out under the following conditions: angular interval $2° \leq 2\theta \leq 70°$, step size 0.02°, spectral recording rate 3 deg/min^{-1}. Identification of the phase composition of the samples was conducted with the PDXL software package (Rigaku corporation) using Powder Diffraction File™ (PDF®) of the Powder

X-ray Standards International Center for Diffraction Data ICDD (PDF 2008).

The specific surface area (S_{sp}) of the studied powders was measured using the Brunauer–Emmett–Teller (BET) method on a TriStar II 3020 automated sorption unit (Micromeritics). The temperature of preliminary degassing of clay material samples was 350°C.

The granulometric composition of the original and modified samples of clay material was determined by laser diffraction using an S-3500 laser granulometer (Microtrac). Before measurements, the aqueous suspension was subjected to ultrasonic treatment for 30 s in a built-in sample preparation unit with an ultrasonic dispersant.

RESULTS AND DISCUSSION

The results of studying the granulometric composition of the powders showed a decrease in the particle size of the clay material with increasing grinding time (Fig. 2).

Based on the shape and height of the maximum, these systems showed a bimodal nature of the grain size distribution. In the G-0 sample, the maximum of the first mode is not clearly expressed and is in the range of 2–5 μm. The second mode is more intense and is recorded in the range of 20–30 μm. As the grinding time of the powders increases, the maximum shifts towards the smallest particle size values.

The median particle size D_{50} for the initial sample is ~11 μm. After 8 h of grinding, this value was 5.3 μm (Table 3). As the grinding time increases, an increase in the number of particles with a size <1 μm is also detected. In samples G-0 and G-8, the content of such particles was 0.7 and 1.6%, respectively.

Analysis of the SEM results (Fig. 3) G-0 indicates the presence of several mineral phases, as evidenced by the different shapes of the particles: flaky and granular. The range of particle sizes is quite wide and ranges from <1 to 300 μm. In sample G-8, particles smaller than 30 μm are detected. The data obtained are in good agreement with the results of studying the granulometric composition of powders using laser diffraction. In samples G-4 and G-8, there are more agglomerates, the formation of which is the result of particle adhesion, which corresponds to the second maximum in the corresponding grain distribution (Fig. 2).

Textural differences between the original and activated samples begin to appear after 1 h of grinding.

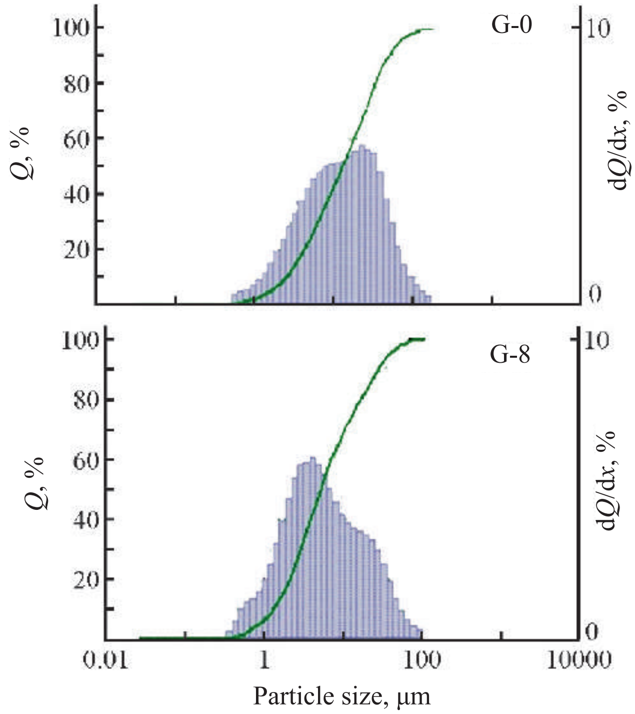

Fig. 2. Schemes of grain distribution for particles of samples of the initial clay material (G-0) and the catalyst produced based thereon during grinding for 8 h (G-8).

Table 4. Texture characteristics of the studied catalyst samples

Time of mechanical activation of clay material, h	Specific surface area according to the one-point Brunauer–Emmett–Teller method, m^2 g^{-1}	Total pore volume, cm^3 g^{-1}	Average pore diameter, Å (±5%)
Original sample	39 ± 2	0.055 ± 0.003	57 ± 3
1	40 ± 2	0.062 ± 0.003	63 ± 3
2	38 ± 2	0.064 ± 0.003	68 ± 3
4	39 ± 2	0.071 ± 0.004	75 ± 4
8	34 ± 2	0.072 ± 0.004	85 ± 4

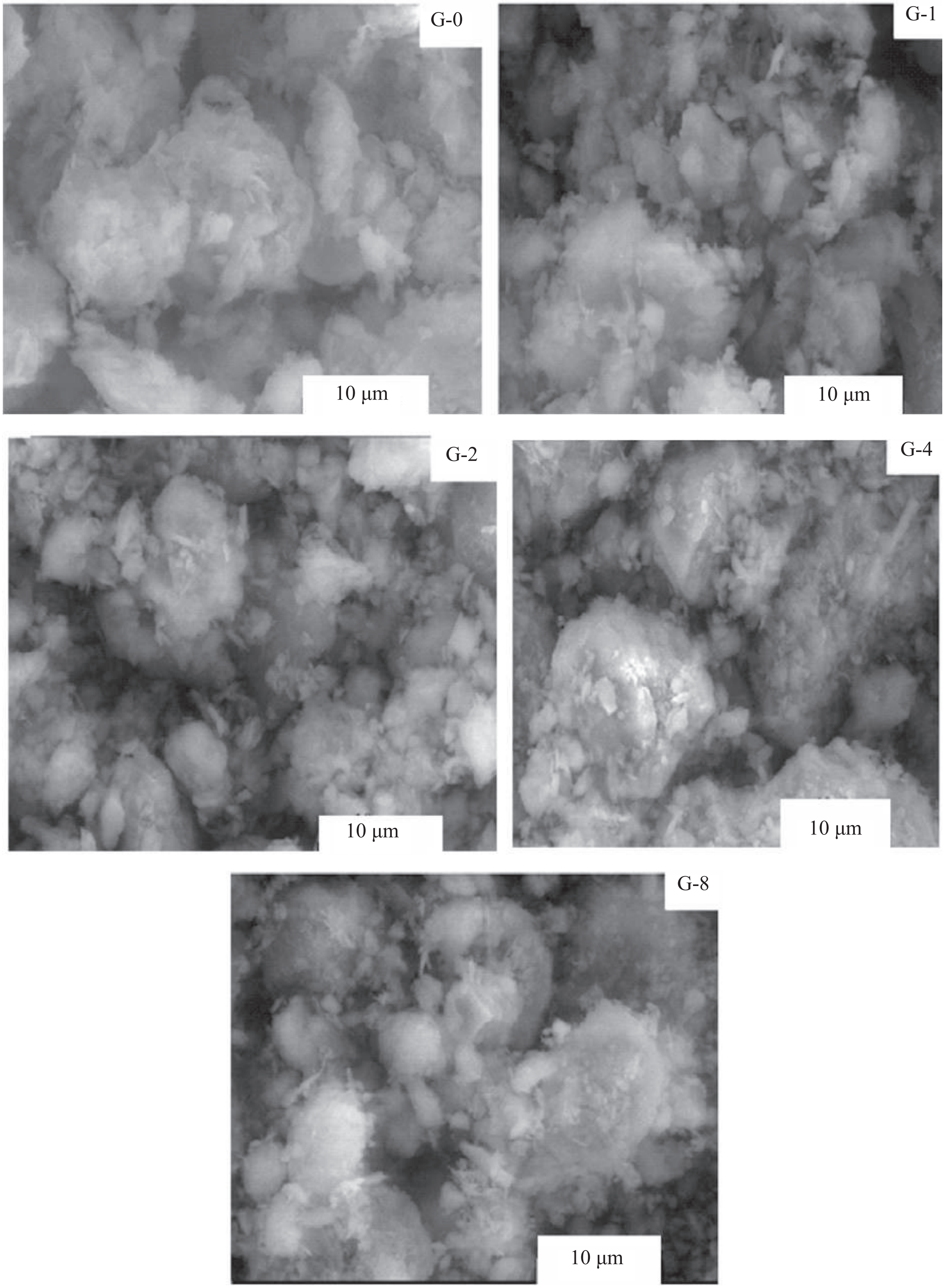
G-0
10 µm
G-1
10 µm
G-2
10 µm
G-4
10 µm
G-8
10 µm

Fig. 3. Microphotographs of the original clay material (G-0) and catalysts based thereon during the grinding process for 1, 2, 4 and 8 h (G-1, G-2, G-4, G-8), obtained by scanning electron microscopy .

Table 5. Acid-base properties of clay material under conditions of mechanical activation and the yield of polypropylene degradation products in the presence of the produced catalysts

Time of mechanical activation of clay material, h	Total content of active sites $\Sigma q\text{p}K_\text{a}^x$, mmol g^{-1}	Hammett acidity function H_0	Yield of liquid products, wt %
Original sample	100.8	2.0	34.0 ± 0.7
1	74.69	3.7	28.0 ± 0.6
2	45.06	3.7	45.0 ± 0.9
4	42.92	5.8	34.0 ± 0.6
8	62.37	5.9	53.0 ± 1.0

The total pore volume and their average diameter increase with grinding time (Table 4).

The obtained isotherms of low-temperature nitrogen adsorption are of the same type for samples G-0, G-1, G-2, and G-4 and belong to type IV according to the IUPAC classification, characteristic of mesoporous bodies [20]. After 8 h of grinding the sample, the adsorption isotherm becomes closer to type III, corresponding to adsorption on non-porous bodies when adsorbate is weakly bound to the surface of the sorbent.

The shape of the hysteresis loops on the isotherms of samples G-0, G-1, G-2 can be attributed to H3 type, which is typical of systems consisting of lamellar particles with slit-shaped pores. The hysteresis loop on the G-0 adsorption isotherm is characterized by the greatest width. The remaining curves are characterized by narrower loops, and their width decreases as the grinding time of the studied samples increases. G-4 has a hybrid hysteresis loop, which can be defined as type H1, characteristic of particles that are fairly equal in size and uniformly packed. It is likely that the particle size distribution became much more uniform after 4 h of grinding. Sample G-8 obviously retained only a residual amount of mesopores; there is no pronounced hysteresis loop on the isotherm. This fact evidences the predominance of the adhesion process under the action of adhesive forces due to an increase in the internal energy of highly dispersed particles over the dispersion process under mechanical action [21].

The XRD patterns showed a change in the intensity of many reflexes without their expansion with a decrease in the size of the fractions, which indicates a progressive amorphization of the structure of the clay material components under mechanical action. This effect is especially pronounces for maxima corresponding to quartz.

Mechanical action has a significant impact on the content of active sites on the surface of catalyst samples. According to the scheme of distribution of active acid-base sites, the surface of the studied samples is characterized by the presence of Brønsted basic (pK_a^x from 7 to 12.8) and acidic (pK_a^x from 0 to 7) sites (Fig. 4).

In the series G-0, G-1, G-2, G-4, there is a decrease in the total number of active sites (Table 5). After 8 h of grinding the clay material, an increase in this indicator is detected, which is 62.37 mmol g^{-1}. With increasing the grinding time of the catalyst powder there is a decrease in the concentration of active sites with pK_a^x values of 0.8–3.5 (Fig. 4), and the H_0 value changes from 2.0 to 5.9. Samples G-4 and G-8 are characterized as materials of average acidity.

In experiments on the thermal conversion of polyethylene and polypropylene without a catalyst under the given experimental conditions, the formation of liquid products was not detected [4, 22]. In this regard, thermal degradation of polymers was not carried out in this study; only experiments on thermocatalytic conversion were conducted in the presence of the

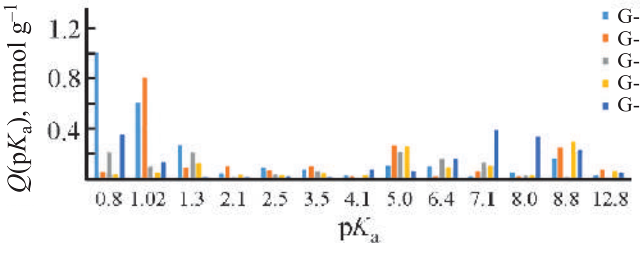

Fig. 4. Distribution of adsorption sites on the surface for the original clay material (G-0) and the resulting catalysts based thereon during the grinding process for 1, 2, 4, and 8 h (G-1, G-2, G-4, G-8).

original and modified samples of clay material. Note that a change was made to the methodology for preparing reaction mixtures: *m*-xylene, previously used as a solvent, was replaced with motor oil.

The results of the study carried out on the degradation of polyolefins showed that all the studied catalysts are not capable of converting a polyethylene–motor oil mixture into liquid hydrocarbons. However, during the conversion, the formation of solid yellow oily products was observed on the walls of the catalytic reactor. Further studies were aimed at studying the conversion of the polypropylene–motor oil mixture.

Analysis of the data obtained showed that in the presence of all studied catalyst samples, conversion of the polypropylene and motor oil mixture into liquid hydrocarbons occurs (Table 5). This difference in results for the degradation of polyethylene and polypropylene is probably due to the peculiarities of their structure. Since every second carbon atom in the macrochain of polypropylene is tertiary, the strength of carbon–carbon bonds in the polypropylene molecule is lower than in the case of polyethylene. In addition, side chain methyl groups increase the effective cross-section of polypropylene molecules compared to polyethylene chains, which promotes better interaction with active sites located inside the pores [23].

For the series of catalysts under study, there is a tendency for the yield of liquid hydrocarbons to increase with increasing grinding time. The maximum amount of target products was produced in the degradation of polypropylene and motor oil with sample G-8; the yield was 53 wt %. It should be noted that during the conversion of this mixture in the presence of G-1 and G-4, there is a decrease in the yield of the liquid fraction compared to the sample of the original material. It can be assumed that during the degradation of polypropylene and motor oil engaging G-1 and G-4, the formation of more gaseous or heavier hydrocarbons is possible, but such products were not studied in this work.

Upon increasing the grinding time of the clay material, as demonstrated above, there is a decrease in the concentration of strongly acidic sites, which, according to the literature, contribute to the formation of gaseous hydrocarbons, and minor changes in the concentration of sites of medium strength. Apparently, it is the change in the acidity spectrum that affects the yield of target products. For comparison, we can cite previously obtained data on the degradation of polypropylene using synthetic amorphous aluminosilicates as catalysts. These catalysts have the same set of acid sites in the pK_a^x range of 3.5–5.0 and exhibit comparable efficiency in the conversion of polymers into liquid hydrocarbons [4].

CONCLUSIONS

By means of mechanical activation, it is possible to produce effective catalysts for the conversion of a mixture of polypropylene and motor oil based on clay material with increased selectivity for liquid hydrocarbons, which have low cost and meet the principles of “green chemistry”. Fine grinding of clay powders induces a change in the catalytic properties of the materials under study and, as a result, contributes to an increase in the yield of target products from 34 to 53 wt %. The ability of aluminosilicates to convert polypropylene into liquid hydrocarbons depends on the number and availability of acid sites of a certain strength. The investigated degradation of polyolefin can also be considered as an alternative method for recycling spent motor oil.

Further study of the degradation of polypropylene may be promising, since changing the reaction conditions, in particular the ratio of polymer : motor oil : catalyst, can lead the desired result: the formation of liquid hydrocarbon products.

ACKNOWLEDGMENTS

The research was carried out using the scientific equipment of the Center for Collective Use “Technologies and Materials” of the Belgorod State National Research University.

AUTHOR CONTRIBUTION

O. E. Lebedeva: formulation of problems, analysis and processing of the results obtained, analysis of literature data; L.V. Furda: selection of research objects, analysis of literature data, conducting experiments on thermocatalytic degradation; preparation of the section Results and Discussion; O.G. Isakulov: preparation of raw materials, production of catalysts based on clay material, carrying out studies of the acid-base properties of the surface of samples of clay material and catalysts based thereon.

FUNDING

This work was supported by ongoing institutional funding.

No additional grants to carry out or direct this particular research were obtained.

CONFLICT OF INTEREST

The authors declare that there are no conflicts of interest

REFERENCES

1. Marcilla, A., Gomez-Siurana, A., and Berenguer, D., *Appl. Catal. A: General,* 2006, vol. 301, pp. 222–231. https://doi.org/10.1016/j.apcata.2005.12.018
2. Obali, Z., Sezgi,, N.A., and Doğu, T., *Chem. Eng. J.,* 2008, vol. 196, nos. 1–2, pp. 116–130. https://doi.org/10.1080/00986440802301537
3. Furda, L.V., Ryl′tsova, I.G., and Lebedeva, O.E., *Russ. J. Appl. Chem.*, 2008, vol. 81, pp. 1630–1633. https://doi.org/10.1134/S1070427208090292
4. Furda, L.V., Smal'chenko, D.E., Titov, E.N., and Lebedeva, O.E., *Izv. vuzov. Khimiya Khim. Tekhnologiya,* 2020, vol. 63. no. 2, pp. 85–89. https://doi.org/10.6060/ivkkt.20206306.6202
5. Li, K., Lei, J., Yuan, G., Weerachanchai, P., Wang, J.-Y., Zhao, J., and Yang, Y., *Chem. Eng. J.,* 2017, vol. 317, pp. 800–809. https://doi.org/10.1016/j.cej.2017.02.113
6. Budsaereechai, S., Hunt,, A.J., and Ngernyen, Y., *RSC Adv.,* 2019, vol. 9, pp. 5844–5857. https://doi.org/10.1039/C8RA10058F
7. Peng, Y., Wang, Y., Ke, L., Dai, L., and Wu, Q., Cobb, K., Zeng, Y., Zou, R., Liu, Y., Ruan, R., *Energy Convers. Manag.*, 2022, vol. 254, ID 115243. https://doi.org/10.1016/j.enconman.2022.115243
8. Fadillah, G., Fatimah, I., Sahroni, I., Musawwa, M.M., Mahlia, T.M.I., and Muraza, O., *Catalysts,* 2021, vol. 11, no. 7, ID 837. https://doi.org/10.3390/catal11070837
9. Krylov, O.V., *Geterogennyi kataliz* (Heterogeneous Catalysis), Moscow: Akademkniga, 2004.
10. Battalova, Sh.B., *Fiziko-khimicheskie osnovy polucheniya i primeneniya katalizatorov i adsorbentov iz bentonitov* (Physico-Chemical Basis for the Production and Use of Catalysts and Adsorbents from Bentonites), Alma-Ata: Nauka, 1986.
11. Komadel, P., *Appl. Clay Sci.,* 2016, vol. 131, pp. 84–99. https://doi.org/10.1016/j.clay.2016.05.001
12. Elhadj, Y.M.S., Perrin, X.F., *Appl. Clay Sci.,* 2021, vol. 213, ID 106250. https://doi.org/10.1016/j.clay.2021.106250
13. Filipović-Petrović, L.M., Kostić-Gvozdenović, L., Erić-Antonić, S.C., *J. Serb. Chem. Soc.,* 2002, vol. 67, no. 11, pp. 753–760. https://doi.org/10.2298/JSC0211753F
14. Hrachová, J., Komadel, P., Fajnor, V.Š., *Mater. Lett.,* 2007, vol. 16, no. 61, pp. 3361–3365. https://doi.org/10.1016/j.matlet.2006.11.063
15. Valera-Zaragoza, M., Agüero-Valdez, D., Lopez-Medina, M., Dehesa-Blas, S., Navarro-Mtz, A.K., Avalos-Borja, M., Juarez-Arellano, E.A., *Adv. Powder Technol.,* 2021, vol. 32, no. 2, pp. 591–599. https://doi.org/10.1016/j.apt.2021.01.004
16. Leite, L., Stonkus, V., Edolfa, K., Ilieva, L., Plyasova, L., Zaikovskii, V., *Appl. Catal. A: General,* 2006, vol. 311, pp. 86–93. https://doi.org/10.1016/j.apcata.2006.06.006
17. Romanenko, E.P., Taraban, E.A., Tkachev, A.V., *Russ. Chem. Bull.,* 2006, vol. 55, no. 6, pp. 993–998. https://doi.org/10.1007/s11172-006-0368-y
18. Tanabe, K., *Solid Acids and Base. Their Catalytic Properties,* New York: Acad. Press, 1970.
19. Lur'e Yu. Yu., *Spravochnik po analiticheskoi khimii* (Handbook of Analytical Chemistry), Moscow: Khimiya, 1989, pp. 190–213.
20. Gregg, S.J. and Sing, K.S.W., *Adsorption Surface Area and Porosity,* London: Academic Press, 1967.
21. Khodakov, G.S., *Fizika izmel'cheniya* (Physics of Grinding), Moscow: Nauka, 1972.
22. Furda, L.V., Krivenko, L.A., and Lebedeva, O.E., *Izv. Vuzov. Khimiya i Khim. Tekhnologiya,* 2005, vol. 48, no. 11. pp. 60–63.
23. Aguado, J., Sotelo, J.L., Serrano, D.P., Calles, J.A., Escola, J.M., *En. Fuels,* 1997, vol. 11, no. 6, pp. 1225–1231. https://doi.org/10.1021/EF970055V

Publisher's Note. Pleiades Publishing remains neutral with regard to jurisdictional claims in published maps and institutional affiliations.